Korean J. Chem. Eng., **28**(11), 2202-2205 (2011)
DOI: 10.1007/s11814-011-0102-9

The effect of graphene nanosheets as an additive for anode materials in lithium ion batteries

Jae Hun Jeong*, Dong-Won Jung*, Byung-Sun Kong, Cheol Min Shin***, and Eun-Suok Oh*,†**

*School of Chemical Engineering & Bioengineering, University of Ulsan, Daehak-ro 102, Nam-gu, Ulsan 680-749, Korea
**KCC Central Research Institute, 83 Mabook-dong, Giheung-gu, Yongin, Gyeonggi-do 446-912, Korea
***Research Center, N-Baro Tech Co., 974-1 Goyeon-ri, Ungchon-myon, Ulju-gun, Ulsan 689-871, Korea
(*Received 17 December 2010 • accepted 14 April 2011*)

Abstract–A small amount of graphene nanosheets was added to commercial graphite as an anode active material in lithium ion batteries and its effects were examined through a variety of physical and electrochemical characterization techniques: FE-SEM, XRD, Raman, BET, and EIS. Compared to a commercial graphite electrode, a composite electrode containing 1 or 5 wt% graphene nanosheets showed higher reversible capacity and enhanced cyclability. This was attributed to the large surface area and low charge transfer resistance of the graphene nanosheets.

Key words: Lithium Ion Batteries, Anode Active Materials, Graphene Nanosheets, Composite Electrodes

INTRODUCTION

Electric vehicles (EVs) have attracted attention as eco-friendly transportation alternatives because they do not emit greenhouse gases during operation and therefore do not contribute to problems of global warming. Polymer electrolyte membrane fuel cells (PEMFCs) and rechargeable lithium ion batteries (LIBs) are investigated as power sources for EVs due to high power density and efficiency. However, PEMFCs require expensive Pt catalysts and the current hydrogen infrastructure is insufficient. Consequently, LIBs are a leading candidate for use as power sources in EVs.

LIBs are widely used in mobile devices, such as cell phones or laptops and in hybrid EVs, due to their high energy density and long cycle life. Graphite is used as an anode material for LIBs due to its high charging/discharging efficiency, low volume change, stable cycle performance, and acceptable specific capacity of 372 mAh g^{-1} [1]. However, the capacity of graphite is insufficient for use in EVs. Therefore, attention has been given to finding new high capacity anode materials, such as tin, silicon, or their composites [2-6]. Unfortunately, metallic active materials undergo very large volume changes during the charge/discharge process and suffer from rapid capacity fading.

Graphene nanosheets (GNSs) have potential for use in high capacity anode materials due to the larger space available for lithium ion intercalation [7-9]. Recently, Guo et al. [10] reported that GNSs showed a reversible capacity of 672 mAh g^{-1} and excellent cycle performance. The lithium storage properties of disordered GNS were also investigated by Pan et al. [11]. They reported that disordered GNS showed reversible capacities of 794-1,054 mAh g^{-1} and good cyclic performance due to increased lithium storage sites, such as edges and defects. However, the density of GNS is too low to be used as a sole anode active material. Rather, nanosheets can be employed as an additive to other high-density materials for commercial use.

In this work, a small amount of GNSs was employed with commercial graphite as anode active materials. A composite electrode was prepared by ball milling and its physical and electrochemical characteristics were investigated using various characterization techniques: field emission scanning electron microscopy (FE-SEM), X-ray diffractometry (XRD), Raman spectroscopy, and electrochemical impedance spectroscopy (EIS). Coin half-cell tests were also conducted to examine the reversible capacity and cyclability of the composite.

EXPERIMENTAL

GNSs that were manufactured by thermal expansion of expandable graphite were provided by N-Barotech Co., Ltd. (Korea). A small amount of GNS was ball-milled for 1 hr with commercial natural graphite (NG; Sodiff Co., Korea). Two composites materials composed of 1 wt% GNS and 99 wt% NG; and 5 wt% GNS and 95 wt% NG; were prepared. Their electrochemical evaluations were measured by CR2016 type, coin half-cells with a composite as a working electrode and lithium metal was used as a reference electrode. A working electrode slurry was prepared by mixing a 85 wt% composite with 5 wt% vapor growth carbon fiber, and 10 wt% polyvinylidene fluoride (Solef 5130, Belgium) binder with n-methylpyrrolidone solvent. Then, the slurries were coated on copper foil with a doctor blade. The electrode sheet was dried in a convection oven at 130 °C for 30 min and a vacuum oven at 80 °C for 12 hr before being assembled in a glove box in an argon atmosphere. The electrolyte in the CR2016 cell was a 1 M $LiPF_6$ (Panaxetec Co., Korea) dissolved in a 1 : 1 : 1 (v/v/v) mixture of ethylene carbonate, ethyl methyl carbonate and dimethyl carbonate. The cells were galvanostatically charged and discharged in 0.005-1.0 V.

The GNS morphology was characterized by FE-SEM (JEOL, JSM-6500F). The specific surface area was measured by a BET (Micromeritics Inc., ASAP2020) system. A Raman spectrometer (Renishaw Pic, iN-Vin) and X-ray diffractometer (Rigaku, RAD-

†To whom correspondence should be addressed.
E-mail: esoh1@ulsan.ac.kr

3C) were employed to determine the crystal structural characteristics of the GNS and NG. The Raman spectra were measured using a Raman spectrometer with a 632.8 nm laser. The XRD analysis was performed with a Cu kα (λ=1.541 Å) X-ray source at an operating voltage of 35 kV. The XRD patterns were collected in the range of 10-80° with a scan rate of 3° min^{-1}.

RESULTS AND DISCUSSION

FE-SEM was conducted to examine the surface morphologies of GNS and NG, and the resulting images are shown in Fig. 1. The image of NG in Fig. 1(a) shows both bulk and flake shapes mixed with a diameter of approximately 10-20 nm and a length less than 10 μm. Fig. 1(b) and 1(c) show the cross-section and surface images of GNS. In the stacked GNS, empty space was observed due to high temperature thermal expansion. BET analysis confirmed that the surface area of GNS was 801.84 m^2 g^{-1}, which was much greater than that of graphite (0.83 m^2 g^{-1}). In general, lithium ions were bound to the surfaces of graphene sheets, the edges and in empty space. Therefore, the GNS could enhance the lithium storage capacity in LIBs compared to NG. A wrinkled structure, typically observed in GNS, was also observed on the surface of GNS, as shown in Fig. 1(c). A small amount of GNS in the anode active materials leads to a decrease in contact resistance between graphite particles and thus increases the electrical conductivity of the electrode.

The XRD pattern of GNS was compared to that of NG in Fig. 2. A diffraction peak of NG at 2θ=26° corresponds to the (002) crystalline plane of graphite (JCPDS card no. 75-1621), whereas a broad diffraction peak at 2θ=17.2° was related to the flakes of NG shown in Fig. 1(a). This diffraction peak shifted to 2θ=20° in the GNS. Therefore, the d-spacing of the (002) crystalline plane of graphite increases according to Bragg's diffraction law. The d-spacing of GNS and NG calculated by the XRD results were 0.225 nm and 0.176 nm, respectively. Other structural differences between GNS and NG were observed by Raman spectra, as displayed in Fig. 3. The G-band peaks near 1,580 cm^{-1} were attributed to the vibration mode of the sp^2 graphite structure and the D-band near 1,335 cm^{-1} was assigned to disordered graphite, such as defects [12]. In addition, the degree of crystallinity of GNS and NG was identified from the relative ratio of the D-band intensity (I_D) to the G-band intensity (I_G). The intensity ratios (I_D/I_G) were 0.69 for NG and 0.96 for GNS, respectively. A higher intensity ratio indicates a higher defect concentration compared to the sp^2 graphite structure, and thus a lower degree of crystallinity due to the high temperature thermal expansion of graphite, which increases the concentration of defects in the graphite structure.

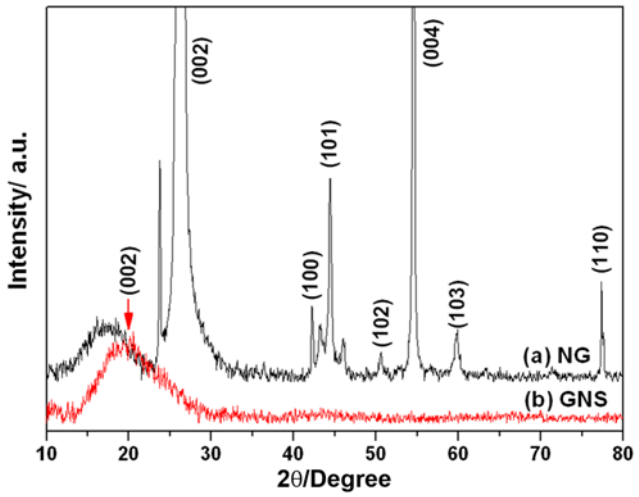

Fig. 2. X-ray diffraction patterns of NG and GNS.

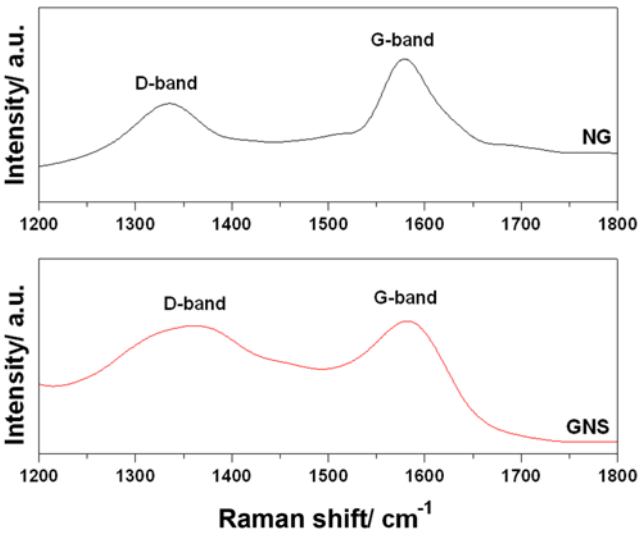

Fig. 3. Raman spectra of NG and GNS.

The electrochemical characteristics of the composite electrodes were investigated using EIS and coin cell tests. The first charge/discharge capacities of the composite electrodes versus voltage (vs. Li/Li^+) are shown in Fig. 4(a). As expected from the XRD and Raman spectra in Figs. 2 and 3, an increase of GNSs in the electrode decreases the crystallinity of the active material in the electrode, and thus gradually decreases the capacity assigned to the low voltage region. Alternatively, the electrodes containing GNS display larger

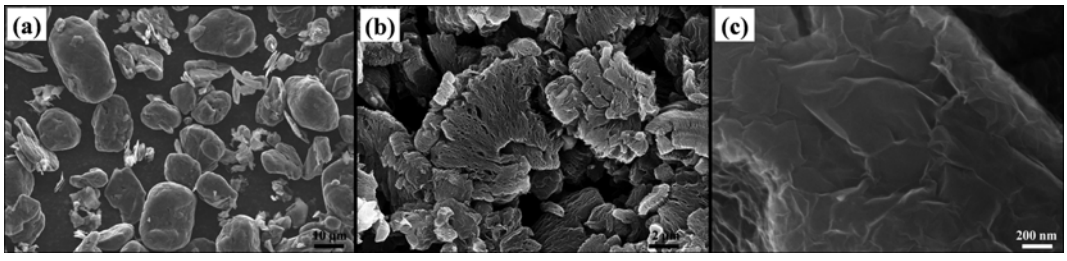

Fig. 1. FE-SEM results of NG and GNS. (a) NG, (b) cross section of GNS, and (c) surface of GNS.

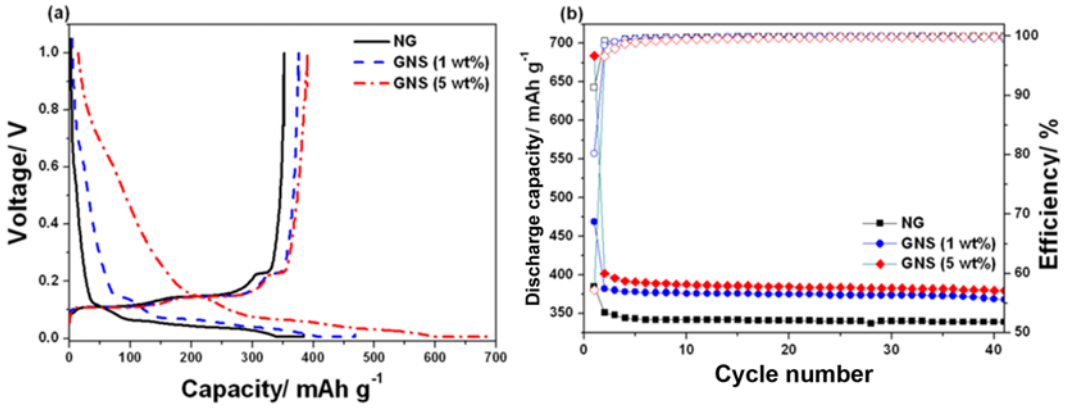

Fig. 4. (a) Voltage versus first charge-discharge capacity and (b) discharge capacities and Coulombic efficiencies of the composite electrodes with cycle number.

voltage hysteresis between discharge and charge curves than the graphite electrode, which is similar to non-graphitic carbon with lower crystallinity than graphite [10,13,14]. As the amount of GNS in the electrode increases, more lithium ions are intercalated in the electrode due to a very high surface area of GNS exhibited by BET analysis, while a more solid electrolyte interface (SEI) can be formed on the electrode surface of the GNSs [15]. An increase in the voltage plateau near 0.67 V in Fig. 4(a) caused a gradual Coulombic efficiency decrease; 91.3% for the electrode without GNS, 80.2% for the 1 wt% GNS electrode, and 57.2% for the 5 wt% GNS electrode based on the discharge and charge curves.

Both the discharge capacity and Coulombic efficiency of the composite electrode versus cycle number are displayed in Fig. 4(b). The electrochemical measurements of the coin-type half cell were performed between 0.005 and 1.0 V at a current density of 0.5 C. As previously mentioned, an increase in the GNS increases the first discharge capacity by providing more sites to absorb the lithium ions, such as edge and defects [16]; 385 mAh g^{-1} for graphite only, 469 mAh g^{-1} for the 1 wt% GNS active material, and 684 mAh g^{-1} for the 5 wt% GNS active material. Alternatively, all three composite electrodes showed very stable cyclic retention up to 40 cycles. At the 40th cycle, their reversible capacities were 339 mAh g^{-1} for NG, 369 mAh g^{-1} for 1 wt% GNS, 380 mAh g^{-1} for 5 wt% GNS and their efficiencies were greater than 99.5%.

The results of the EIS of the composites are shown in Fig. 5. As the amount of GNS in the electrode increases, the size of the semicircle in the medium frequency region significantly decreases. The semicircle in the medium frequency was ascribed to the charge transfer process at the interface between the electrode and electrolyte [10,17,18]. Therefore, the increase of GNS in the electrode decreases the charge transfer resistance. As previously mentioned, the GNS was more spacious and thus lithium ions were more easily transferred to the GNS than in graphite. Additionally, since the electron transfer in the electrode can affect the rate of the charge-transfer reaction at the interface, the EIS result indirectly indicates the possibility for enhancing the electronic conductivity by adding a small amount of GNS in the graphite. This is proven by measuring the sheet resistance of the electrode (CMT-100M, AIT. Co., Ltd.). As expected from the EIS spectra, the sheet resistance decreased with increasing GNS in the electrode; 665.9 mΩ/sq for graphite only, 511.6 mΩ/sq for the 1 wt% GNS active material, and 188.8 mΩ/sq for the 5 wt% GNS active material.

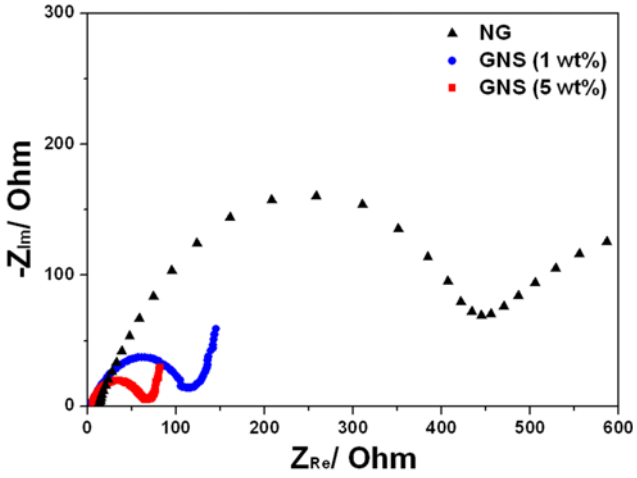

Fig. 5. Electrochemical impedance spectra of the composite electrodes.

CONCLUSIONS

The physical and electrochemical characteristics of composite electrodes with a small amount of graphene nanosheets were compared using commercial natural graphite as an anode active material in lithium-ion batteries. The layered graphene morphology provides more active sites for lithium ion intercalation, such as edges and defects, and ultimately increases the reversible capacity of the electrode even when only a very small amount of graphene nanosheets are used in the electrode. In addition, the graphene nanosheets contribute to a decrease in the charge transfer resistance resulting from the improvement of lithium ion diffusion, as well as electronic conductivity.

ACKNOWLEDGEMENTS

This research was supported by the Basic Science Research Program through the National Research Foundation of Korea (NRF)

funded by the Ministry of Education, Science and Technology (2010-0015257, 2010-0024077).

REFERENCES

1. Y. C. Chen, J. M. Chen, Y. H. Huang, Y. R. Lee and H. C. Shih, *Surf. Coat. Technol.*, **202**, 1313 (2007).
2. H. Zhao, C. Jiang, X. Hea, J. Ren and C. Wan, *Electrochim. Acta*, **52**, 7820 (2007).
3. X. Wang, Z. Wen, Y. Liu and X. Wei, *Electrochim. Acta*, **54**, 4662 (2009).
4. A. Fernández, F. Martín, J. Morales, J. R. Ramos-Barrado and L. Sánchez, *Electrochim. Acta*, **51**, 3391 (2006).
5. A. Shukla, R. Kumar, J. Mazher and A. Balan, *Solid State Commun.*, **149**, 718 (2009).
6. B. J. Jeon, S. W. Kang and J. K. Lee, *Korean J. Chem. Eng.*, **23**, 854 (2006).
7. S. Yang, H. Song and X. Chen, *J. Power Sources*, **173**, 487 (2007).
8. F. Ji, Y. Li, J. Feng, D. Su, Y. Wen, Y. Feng and F. Hou, *J. Mater. Chem.*, **19**, 9063 (2009).
9. X. Wang, Z. Zeng, H. Ahn and G. Wang, *Appl. Phys. Lett.*, **95**, 183103 (2009).
10. P. Guo, H. Song and X. Chen, *Electrochem. Commun.*, **11**, 1320 (2009).
11. D. Pan, S. Wang, B. Zhao, M. Wu, H. Zhang, Y. Wang and Z. Jiao, *Chem. Mater.*, **21**, 3136 (2009).
12. A. C. Ferrari and J. Robertson, *Phys. Rev. B.*, **61**, 14095 (2000).
13. D. Larcher, C. Mudalige, C. M. Gharghouri and J. R. Dahn, *Electrochim. Acta*, **44**, 4069 (1999).
14. Y. P. Wu, C. Jiang, C. Wan and R. Holze, *Electrochem. Commun.*, **4**, 483 (2002).
15. J. Yao, G. X. Wang, J. H. Ahn, H. K. Liu and S. X. Dou, *J. Power Sources*, **114**, 292 (2003).
16. S. R. Mukai, T. Hasegawa, M. Takagi and H. Tamon, *Carbon*, **42**, 837 (2004).
17. S. Yang, J. Huo, H. Song and X. Chen, *Electrochim. Acta*, **53**, 2238 (2008).
18. Q. Pan, K. Guo, L. Wang and S. Fang, *Solid State Ionics*, **149**, 193 (2002).